Natural Hazards (2020) 102:1225–1248
https://doi.org/10.1007/s11069-020-03954-5

ORIGINAL PAPER

A dynamic stability analysis for the Olinalá landslide, northeastern Mexico

Jorge A. Salinas-Jasso[1] · **Juan C. Montalvo-Arrieta**[1] · **José R. Chapa-Guerrero**[1]

Received: 19 March 2019 / Accepted: 18 April 2020 / Published online: 28 April 2020

Abstract
We have evaluated slope stability conditions considering different triggering conditions for the Olinalá landslide, a paleo-landslide located in the northern front of the Sierra Madre Oriental, northeastern Mexico. Models included assessment of the influence of both aseismic (suggesting different groundwater levels) and a strong earthquake shaking scenario. Results suggest the Olinalá landslide is relatively stable even considering a fully-saturated hydrological stage through the slope (e.g., after the impact of major hurricanes), a typical situation in the study area. Considering these circumstances, there is no evidence of a reactivation of the landslide after the impact of hurricanes in the region. Conversely, hazardous scenarios result after evaluate a combined influence of moderate seismicity and extreme hydrometeorological conditions. This study suggests that some geomorphological features observed in northeastern Mexico are unfeasible without considering the effect of earthquakes. Our approach could model the behavior of pseudostable old landslides through the region, in the face of future reactivations and risk situations.

Keywords Landslide hazard · Olinalá landslide · Dynamic stability analysis · Northeastern Mexico · Seismic scenarios

1 Introduction

Landslides have a key influence on landscape change, controlling the geomorphological evolution in mountainous terrains (Korup et al. 2010). Such kind of mass movements are major cause of structural damage and loss of life when interacts in a spatio-temporal scale with population centers, even resulting in more fatalities and damages than those generally reported (Alcántara-Ayala 2002). Landslide hazard has been less quantified in comparison with that induced by other natural hazards as earthquakes, volcanic activity or floodings. Usually, social and economic impacts of landslides are included within the total damage related with the phenomena that induce slopes instability, precluding a real estimation of landslide risk (Bird and Bommer 2004; Petley 2012). Risk is exacerbated in zones where

✉ Jorge A. Salinas-Jasso
j.saja90@gmail.com

[1] Facultad de Ciencias de La Tierra, Universidad Autónoma de Nuevo León, Ex-Hacienda de Guadalupe km 8., Carr. Linares – Cerro Prieto, 67700 Linares, NL, Mexico

coexist landslide prone areas and growing urban settlements, especially in developing countries where the lack of a well-based prevention culture reduces the chances to cope with disasters (Corominas et al. 2014). Hazard assessments have focused on documenting spatial distribution and causal factors of landslides as well as to localize prone slope instability sites (Dai et al. 2002; Fell et al. 2008). Landslide hazard mapping has been enhanced by analysis and data processing of causative factors as thematic layers on GIS platforms and using remote sensing data, depicting a final zonation with different levels of susceptibility or hazard (Carrara et al. 1999; Jibson et al. 2000; Dewitte et al. 2006; Legorreta Paulín et al. 2010; Muñiz-Jauregui and Hernández-Madrigal 2012; Shahabi and Hashim 2015; Murillo-García et al. 2019; Salinas-Jasso et al. 2019b). Some attempts have been made to predict a likely reactivation of ancient landslides (Dewitte et al. 2006; Van Den Eeckhaut et al. 2007; Massey et al. 2013; Villaseñor-Reyes et al. 2018), which may involve high levels of economic loss and catastrophic consequences by the uncertainty related with their origin and behavior (Mansour et al. 2011; Palmer 2017). The analysis of unexpected movement reactivations in old mass bodies still being complicated, especially when instability patterns and displacement rates are unknown and emergency plans are not prepared to deal with the problem. A research concern regarding the reactivation of old slow-motion landslides is to define under what circumstances these events could become devastating, a critical task in high populated areas (Palmer 2017). Documentation of reactivation lapses is often challenging and requires deployment of high precision instruments as inclinometers, GPS stations, piezometers or inspection boreholes (Massey et al. 2013). Several uncertainties should be considered at the time of the analysis. Geometry and mechanism of the landslide, hydrological frame, potential triggers and controls, expected time of failure or reactivation and the potential damage areal extent should be taken account for the development of warning systems (Corominas et al. 2005; Van Asch et al. 2007). However, main limitations rely on economic costs for instrument acquisition and long-term monitoring campaigns, precluding a detailed analysis. Remote sensing techniques, mainly satellite-based methodologies, have been used for monitoring slope movements in landslide-prone areas improving the results achieved by conventional ground-based techniques (Metternicht et al. 2005; Cascini et al. 2010; Casagli et al. 2016; Intrieri et al. 2017).

The Monterrey Metropolitan Area (MMA) has experienced a disordered urban growth during the last 50 years. Urban expansion has increased dramatically occupying high-relief areas, including some dormant landslides like the Olinalá landslide, a creeping and sliding mass on the north flank of the Los Muertos anticline. Although there is not a fully accepted consensus about the origin of this landslide, it has been proposed the mass movement occurred under hydrogeological saturated conditions, as for other similar land and rock masses through the Monterrey Salient (Ruiz Martínez and Werner 1997; Salinas-Jasso et al. 2017). Until now, the ground shaking influence from earthquakes has not been considered as a cause of these paleo-landslides. We have developed five scenarios in order to evaluate stability conditions may lead to a likely failure of the Olinalá landslide and define a landslide hazard assessment for the urban settlements located in the southern part of the MMA. We analyzed the Olinalá landslide in both static (aseismic) and seismic conditions to determine the likelihood of failure caused by changes in groundwater conditions and the influence of strong ground shaking. Understanding the causes that control slope stability conditions through the mass body is a critical step in recognizing and preventing future landslide related disasters in similar or worst expected scenarios. Such a description will allow to define under what scenarios the Olinalá landslide would reactivate as a devastating event, which may be applied for other old and more recent landslides dispersed along the Monterrey Salient trough northeastern Mexico and develop landslide risk assessments.

2 Study area

2.1 Location

The Monterrey Metropolitan Area is the most important urban center in northeastern Mexico. Located in the Nuevo León state, the MMA is formed by several towns including major cities as Monterrey, San Pedro, San Nicolás, Guadalupe, Apodaca, Santa Catarina, Escobedo, García and Santiago. According with the last demographic census carried out by INEGI in 2015, 4.4 million people live in the MMA (INEGI 2019). Main settlements are distributed inside a valley delimited by the Sierra Madre Oriental (SMO) mountains to the south and minor elevation ranges in the north and the east (e.g., Las Mitras, Topo Chico and La Silla hills). The disordered and accelerated urban growth, influenced by low-income jobs, poverty and high rates of industrialization since early the twentieth century, has contributed to a rearrangement of the population density, placing human-irregular settlements on high mountain areas through the MMA (Fig. 1). Besides, constant developing of infrastructure in prone slope instability areas bordering the city and the lack of rigorous lineaments for construction development have adversely impacted the environment. Hurricanes, floodings and landslides are the most recurrent hazards affecting the population in the region. However, recent recording of low to moderate seismicity along the northeastern Mexico has raised social and government concerns for potential structural damage and injuries that this activity could cause throughout the region.

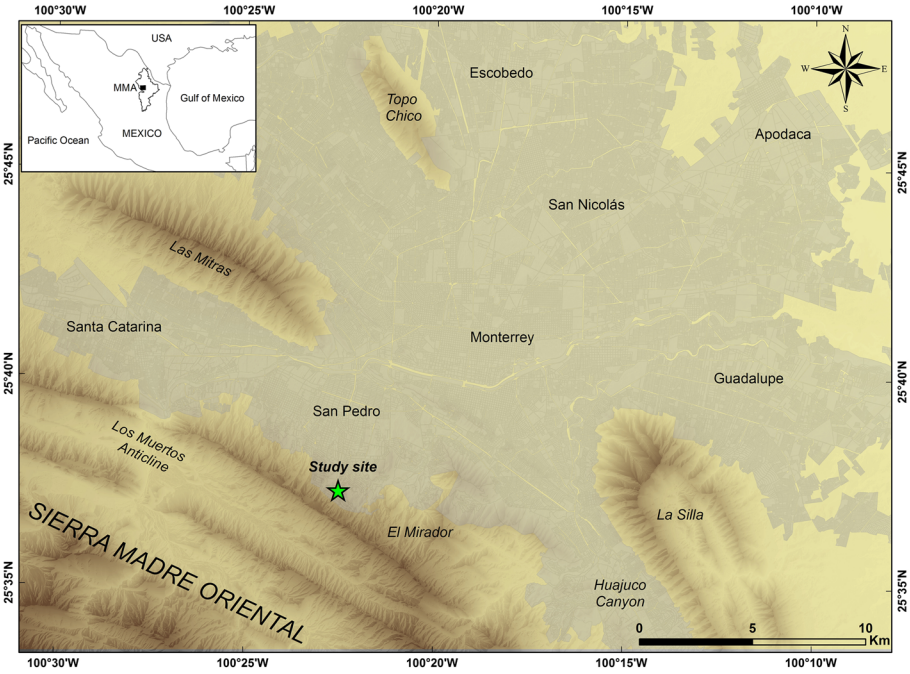

Fig. 1 Location of the Monterrey Metropolitan Area. Gray area depicts the extension of the urban area. Major cities (normal text) and hills (italic text) are defined. The star shows the location of the Olinalá landslide

2.2 Geological frame

The MMA is located in the tectonic front of the Sierra Madre Oriental, a fold-thrust belt formed during the Laramide Orogeny in the Late Cretaceous (Eguiluz de Antuñano et al. 2000). Evolution of the geological and structural pattern of the study area was controlled by a compressive displacement towards the north-northeastern of the sedimentary sequence over evaporite horizons, which was counteracted by structural highs at the late phase of the Laramide deformation. Folds can be traced over distances of up to 60 km and have wavelengths between 4 and 7 km (Padilla y Sánchez 1985). Variations in the shape, wavelength and amplitude of the folds are related to the lithological contrast present in the study area. The SMO outcrops are characterized by upright and tight folds with almost vertical axial planes and limbs slightly overturned towards the northeast. These structures are composed of thick limestones at higher elevations towards a wide transition zone of fine-grained sandstone, siltstone and shale on the foothills (Fig. 2) (Montalvo-Arrieta et al. 2010). Bedrock is fragmented by discontinuities sets forming structural wedges, which define the dimensions and likely failure behavior of the rock slopes (Salinas-Jasso et al. 2017). Quaternary deposits as unconsolidated colluvium, landslide deposits and alluvial sediments overlain discordantly the bedrock. The valley is filled by a thick Cenozoic sequence of unconsolidated sediments of poorly rounded clasts embedded in a fine-grained matrix derived from weathering of clastic and calcareous rocks, forming a floodplain extending towards the northeast (Salinas-Jasso et al. 2019a). The study area is located in the denominated the Monterrey Metropolitan Area aquifer, which has an estimated area of 905 km^2 (CONAGUA 2018). There are two main hydrostratigraphic units in the area: (1) a shallow unconfined aquifer defined by highly permeable alluvial sediments and weathered shales of the Méndez Fm., and (2) a fractured aquifer characterized by the calcareous sequence, which is confined by shales of the Méndez Fm. on the top and evaporites of the Minas Viejas Fm. at the lower limit (De León-Gómez et al. 1998). Small leaky aquifers are distributed along clastic wedges. Aquifer recharge occurs through the overlaying alluvial deposits and is strong dependent on rainfall events, which have large temporal variations throughout the year (CONAGUA 2018). Groundwater level varies due to the topographic contrast between the mountain and the valley. The highest hydraulic heads are recorded in the mountainous

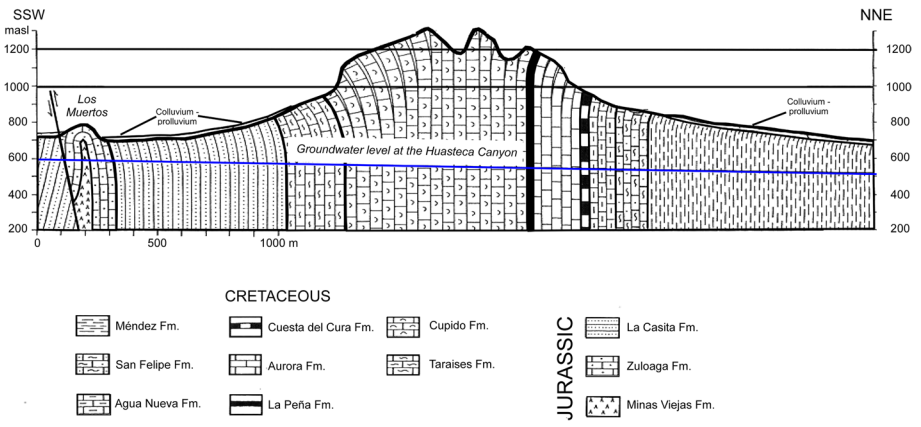

Fig. 2 Stratigraphic section of the north flank of the Los Muertos anticline, east to the Huasteca Canyon. Adapted from Chapa Guerrero (1993)

region with heights reaching 600 m, descending towards northeast. However, there is not updated nor available piezometric data in the study area. CONAGUA, Mexico's water authority, does not has a well coverage of boreholes in the study area, where most of the boreholes are probably private. Therefore, it is practically impossible to continuously monitor and analyze the static and dynamic groundwater levels in the study area.

2.3 Hydrometeorological setting

According to the Köppen climate classification, the MMA climate is semiarid (BSh), characterized by extremely hot temperatures (~40 ºC) and prolonged periods of droughts through the year, especially in the summer. Chilly winters dominate towards the end of the year, with temperatures below the freezing point and snowfall occurrence on hilly zones. Average temperature ranges between 25 ºC and 30 ºC (CONAGUA 2019). Average annual precipitation is approximately of 650 mm, mainly during the rainy-season from July through October. September is the month with the highest rainfall accumulation (~180 mm), which is distributed in lapses up to one-week duration. Rainfall is mainly related to convective systems, characterized by high intensity and short duration storms. Near the hilly region orographic precipitation occurs, affecting only a few isolated zones. Cold fronts are typical between November and February, bringing low temperatures, moisture and precipitation through the entire region.

Because of its geographical position near the Gulf of Mexico, the MMA is constantly impacted by hurricanes and tropical storms formed in the Atlantic Ocean and the Caribbean Sea. During the last 50 years, 45 storms have impacted northeastern Mexico (Jáuregui 2003; Montalvo-Arrieta et al. 2010). These phenomena discharge a large amount of water in short periods (48–72 h), changing drastically the hydrological frame, slope stability conditions, and causing social and economic disasters. Among the storms that have hit northeastern Mexico, four hurricanes stand out by their intensity and the impact generated in the MMA (Table 1): Beulah (1967, Saffir-Simpson scale 4), Gilberto (1988, Saffir-Simpson scale 5), Emily (2005, Saffir-Simpson scale 4) and Alex (2010, Saffir-Simpson scale 2). Precipitations generated by these hurricanes exceeded the annual average rainfall in a few days, causing extensive destruction in infrastructure, catastrophic floods, several landslides, injuries and fatalities (Montalvo-Arrieta et al. 2010). After this, any major hurricane has impacted the study area, only sporadic tropical storms.

A special case was the Hurricane Alex mid-2010, one of the most powerful hurricanes to hit Mexico in the last 40 years (CONAGUA 2010). Alex was the first tropical storm formed during de 2010 Atlantic hurricane season. Alex made landfall in La

Table 1 Major hurricanes that have impacted the MMA in the last 50 years

Hurricane	Date (mm/dd/yy)	Maximum Saffir-Simpson scale	Maximum daily rainfall accumulation (mm)
Beulah	09/22/1967	4	155
Gilberto	09/17/1988	5	260
Emily	07/20/2005	4	248
Alex	07/01/2010	2	315

Data from Montalvo-Arrieta et al. (2010) and CONAGUA (2019)

Pesca, Tamaulipas on June 30 as a hurricane category 2 in the Saffir-Simpson scale, maximum intensity reached during the storm activity. Despite this situation, torrential rainfalls and sustained winds up to 200 km/h were cause of vast damage through northeastern Mexico (CONAGUA 2012). According to the climate data reported by CONAGUA (2019), the maximum rainfall reported during the course of Alex was recorded in the Nuevo León state. On July 1st, 446.5 mm were discharged in a 24 h period through the mountains bordering the southern portion of the MMA (La Estanzuela automatic station). Since the landfall (June 30) and until the hurricane was largely dissipated (July 2), it was recorded 830 mm of water accumulation (CONAGUA 2010), one of the highest rainfall accumulations ever recorded for a hurricane in northeastern Mexico (Fig. 3). Damage was severe across the Nuevo León state. In the MMA, heavy rainfall affected daily routine of the population, completely ceasing educational and productive activities. Serious damage to urban and road infrastructure and thousands of houses, in addition to situations threatening health, telecommunications, energy and water, as well as missing persons and deaths emerged in the aftermath of Alex. However, there is not a detailed inventory of landslides caused by this hurricane or any other for the MMA, which prevents the development of realistic landslide risk assessments for the region.

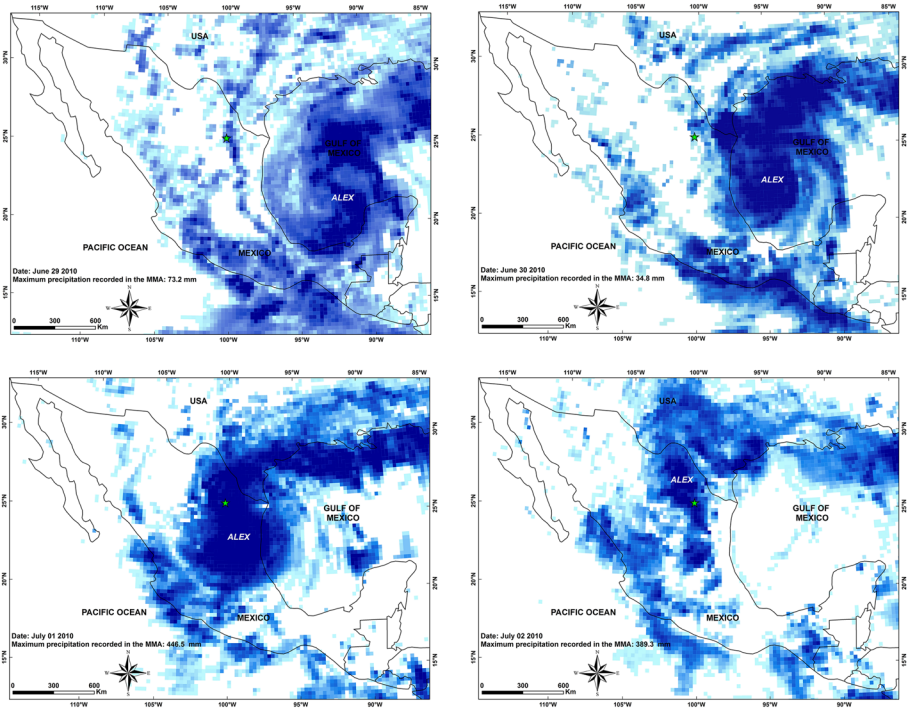

Fig. 3 Evolution of the hurricane Alex (2010) during its pass through the Gulf of Mexico (June 29–June 30), landing in Mexico (July 01) and dissipation (July 02). The start defines location of the MMA. Data from https://pmm.nasa.gov/

2.4 Seismicity

Seismicity is recorded by a relatively young seismic network since 2006 (Ramos-Zuñiga et al. 2012a). Thereafter, low to moderate magnitude earthquakes ($1.9 \leq M \leq 5.0$) have been identified with a random distribution across the region, although some clusters have been monitored near the front of the SMO (Fig. 4) (Ramos-Zuñiga et al. 2012b; Gómez-Arredondo et al. 2016; Montalvo-Arrieta et al. 2015, 2018). A few earthquakes have been reported near the MMA since 1982, where the 2010 San Pedro earthquake (M 4.0) and the 2013 Santa Catarina earthquakes (M 3.3 and 3.7) stand out (Galván-Ramírez and Montalvo-Arrieta 2008; Ramos-Zuñiga et al. 2012a; Salinas-Jasso et al. 2019a). Although no damage was reported for these events, a social concern was evident because of the unusual activity. Otherwise, minor damage in houses and property as well as mass wasting processes were reported from two swarms in neighboring areas of the MMA: the 2012 seismic sequence near the Linares city ($2.5 \leq M \leq 3.6$; Gómez-Arredondo et al. 2016; Salinas-Jasso et al. 2018) and the El Cuchillo seismic sequence ($2.8 \leq M \leq 4.5$; Montalvo-Arrieta et al. 2018). The latter occurred from October 2013 to July 2014 around China, General Terán and Los Ramones cities, 90 km southeast of the MMA. The El Cuchillo seismic sequence, the first case of induced seismicity in northeastern Mexico, has been linked to sudden changes in the water storage of the El Cuchillo dam after the extraordinary rainfalls related to the pass of two hurricanes (Montalvo-Arrieta et al. 2018). Montalvo-Arrieta et al. (2015) estimated macroseismic intensities of MMI VI near the epicentral area and up to MMI V values for some sites in the MMA. These unexpected values in the MMA may have been conditioned by the shallowness (1–20 km) of the earthquakes and the site geological features on which the city is settled above (Salinas-Jasso et al. 2019a). It is important to mention that this seismicity has not generated landslides in the MMA neither a reactivation of the Olinalá landslide.

There is historical evidence of major earthquakes through northeastern Mexico, which suggests a geological context with enough seismogenic potential to produce high intense and destructive earthquakes through the region (García Acosta and Suárez Reynoso 1996; Gálvan-Ramírez and Montalvo-Arrieta 2008). García Acosta and Suárez Reynoso (1996) reported at least 20 earthquakes have shocked northeastern Mexico, inducing slightly to moderate damage in some cities located in the SMO front, including the MMA. The most significant event, in terms of intensity and damage, documented by these authors was the April 28, 1841 earthquake near the Punta Santa Elena community, in the nearby state of Coahuila. This event was felt over a radius of 400 km in major cities like Saltillo, Monterrey, Linares and Victoria (Galván-Ramírez and Montalvo-Arrieta 2008). Due to the lack of instrumentation when this earthquake occurred, the magnitude is unknown. However, according to the reports compiled by García Acosta and Suárez Reynoso (1996) macroseismic intensities could reach maximum values up to MMI VIII in the epicentral zone, which can be related to earthquakes of magnitude $6.0 \leq M \leq 7.0$. If this were true, the 1841 earthquake would be one of the biggest events occurred in the region (Ramos-Zuñiga et al. 2012b). Besides, four major earthquakes have occurred between 1787 and 2006 through northern Mexico and the U.S. border (Galván-Ramírez and Montalvo-Arrieta 2008): the 1887 Bavispe, Sonora earthquake (M 7.4, Natali and Sbar 1982), the 1928 Parral, Chihuahua earthquake (M 6.5, Doser and Rodríguez 1993), the 1931 Valentine, Texas earthquake (M 6.4, Doser 1987) and the 1995 Alpine, Texas earthquake (M 5.7, Xie 1998; Frohlich and Davis 2002).

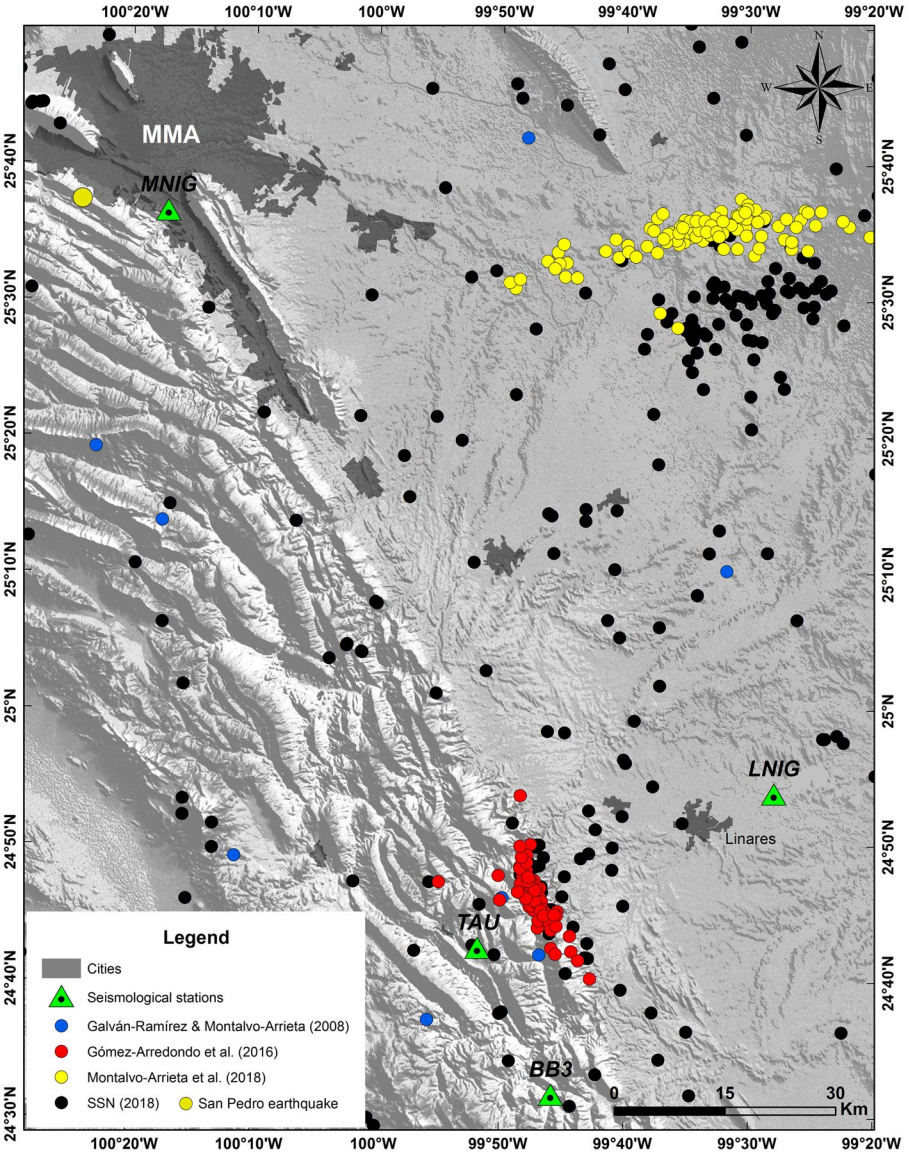

Fig. 4 Seismicity along the northern part of the Sierra Madre Oriental. Historical events (blue circles), instrumental events (black circles) and earthquake swarms (red and yellow circles) are showed. Green circle shows location of the San Pedro 2010 earthquake. Triangles define seismological stations: Monterrey (MNIG), Linares (LNIG), Bosque Escuela (TAU) and Camarones (BB3). Dark gray areas show major cities

Three major fault systems have been postulated in northeastern Mexico: La Babia fault, the San Marcos fault and the Mojave-Sonora megashear. La Babia and the San Marcos faults delimit the Sabinas basin and were originated during the opening of the Gulf of Mexico as normal faults in the Middle Jurassic (Martini and Ortega-Gutiérrez 2018). For these structures have been reported at least two reactivations: one in the Early Cretaceous

and other in the Paleogene (McKee et al. 1984; Chávez-Cabello et al. 2005; Fitz-Díaz et al. 2018). Conversely, the Mojave-Sonora megashear has been proposed as a left-lateral displacement of about 800 km in the Jurassic (Dickinson and Lawton 2001). However, its existence is still quite controversial (Molina-Garza and Iriondo 2005). Regional seismicity has been related to: (a) the reactivation of basement master faults under a compressional regime (Galván-Ramírez and Montalvo-Arrieta 2008; Ramos-Zuñiga et al. 2012b; Gómez-Arredondo et al. 2016), and (b) sudden changes in the water storage of the El Cuchillo reservoir in the Gulf Coastal Plain (e.g., the El Cuchillo seismic sequence, Montalvo-Arrieta et al. 2018).

3 Landslide hazard in the MMA

Regionally, landslides are mainly associated to extraordinary rainfalls. In conjunction, such events have produced several damage including fatalities and disruption of highways along the Sierra Madre Oriental hilly regions. Anthropogenic causes as mining, excavation and overloading of slopes also have been linked with a wide variety of slope failures through the MMA (Montalvo-Arrieta et al. 2010). However, comprehensive information about the occurrence, causes and effects still being scarce for the MMA. Such a situation is reflected in the lack of detailed landslide inventories, the minimum data required to develop a seemly landslide hazard assessment (Guzzetti et al. 2012). Main sources of information are reports by government agencies, mostly incomplete for a specific period or trigger. Data collection through searching on local newspaper archives has constituted a valuable and recurrent tool in the generation of regional landslide databases. However, most of the available information derived from this methodology is generated only for disastrous events (Salinas-Jasso et al. 2017).

Chapa Guerrero (1993) carried out a detailed mapping and geomorphologic analysis in mountainous regions adjacent to Monterrey and San Pedro cities, in the southern side of the MMA. The main result was a six categories landslide hazard map, including safety recommendations and mitigation measures. Montalvo-Arrieta et al. (2010) developed an evaluation of landslides causes and effects through the analysis of geological, structural and climate data. They concluded that rainfall-induced landslides as rockfalls and shallow debris flows are the most recurrent typologies of landslides in hilly regions of the MMA. Salinas-Jasso et al. (2018) reported the first documented case of earthquakes-induced landslides for the Monterrey Salient for the 2012 seismic sequence in the Santa Rosa canyon. Salinas-Jasso et al. (2019b) developed a regional landslide hazard assessment for the MMA predicting the expected areal limits for potential earthquake-induced landslides for postulated shaking scenarios. In their work, the worst scenario postulated was a M 6.5 earthquake and fully-saturated water conditions on regional slopes, the same scenario modeled in our work. Clusters of debris flows and rock avalanches would be expected along the southern part of the SMO, which would involve high hazard conditions in conjunction with the damage by the earthquake itself. A similar approach was developed by Galván-Ramírez and Montalvo-Arrieta (2008) for a hypothetical M 6.5 earthquake in the southeastern segment of the San Marcos fault, in central Coahuila. They calculated ground accelerations for this earthquake, forecasting values up to 50 cm/s^2 in the MMA and several rockfalls through the epicentral area.

Several complex old landslides have been documented along the Monterrey Salient (Ruiz Martínez and Werner 1997). Although these masses are in pseudostable stability

conditions now, it has been documented some traces of very slow reactivations through them (Salinas-Jasso et al. 2017), depicting potentially hazardous conditions specially for those mass bodies that have been covered by urban settlements. Chapa Guerrero (1993) and Montalvo-Arrieta et al. (2010) recognized the presence of ancient landslides in the MMA (e.g., the Olinalá and Las Mitras landslides, respectively). These events are characterized by clastic materials involving argillaceous units and pebbles to huge blocks from calcareous formation. Even though the study area has been constantly impacted by hurricanes, which precipitate significant amounts of rainfall over the time, none of these storms have produced reactivations along these paleo-landslides. However, rock and soil falls, shallow debris flows and slides are frequent along the mass bodies when cyclonic rainfalls hit the region. This evidence exposes a lack of hazard assessments for the study area as well as for the northeastern Mexico. Such projects should be developed as soon as possible in order to implement adequate prevention and mitigation actions for a society increasingly eager to inhabit landslide prone areas of the MMA.

4 The Olinalá landslide

The Olinalá landslide is located at the front of the Monterrey Salient and has been overlain by urban settlements of the San Pedro city, one of the wealthiest towns in the country (Fig. 5a). The study area has become an attractive residential zone by its nearby location to high quality social services and the natural perspective. Chapa Guerrero (1993) was the first to describe the landslide in detail, suggesting an age of activation and a possible triggering cause. The landslide is mainly characterized by a slow creep mass displacing the upper Cretaceous sequence through a rupture surface defined by gravity-driven toppling and a progressive transitional sliding in a NNE direction. The Olinalá mass have an area of about 4.5 km^2 and an estimated volume of 275×10^6 m^3 (Chapa Guerrero 1993). Similar displaced masses are identified around the Olinalá landslide although less extended in dimensions, which could imply a bigger and complex landslide or several pulses of slope instability (Fig. 5b). The scarp of the Olinalá landslide is located at an elevation of approximately 1700 masl on the north side of the Monterrey Salient. Slopes in the upper part of the landslide reach 86º, the steeper surface along the landslide (Fig. 6a). The scarp is developed on a vertical slope affecting massive limestones of the Cupido and Aurora formations, including an intermediate horizon of shales of La Peña formation (Fig. 6b). As it descends topographically, displacement affects a thick sequence of clayey carbonates and shales including chert and organic horizons, represented by the Cuesta del Cura, Agua Nueva and San Felipe formations. Because of their precarious stability conditions, such lithologies are the most susceptible to generate shallow landslides and affect the urban settlements located above the Olinalá landslide. A gentle topography reigns through the deposit zone, even with very flat slopes in the medium zone. Minor landslide scarps are apparent on the transportation zone. Shales of the Méndez Formation constitute the landslide toe with minimum perturbances by the mass movement, but recurrently affected by recent landslides as rockfalls, debris flows and slides due to the precarious geomechanical properties and extraordinary rainfall events. Rock outcrops are covered by thick masses of colluvium and recent landslides. Several huge limestones blocks are located through the landslide mass. These blocks are embedded between clastic and calcareous weathered materials, usually removed during the rainy season. Chapa Guerrero (1993), based on a morphological analysis of the sedimentary sequence, inferred slip surface is formed within the weathering zone of the

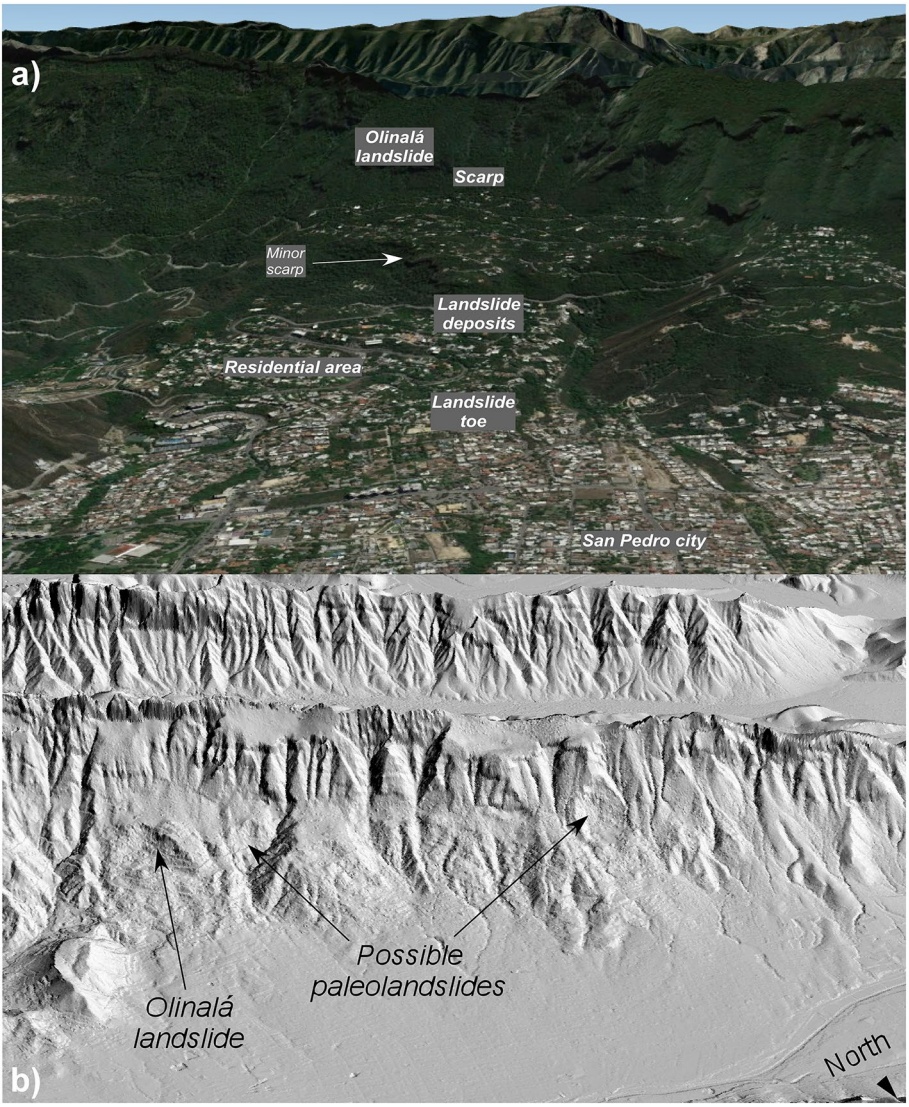

Fig. 5 The Olinalá landslide. **a** Oblique image from Google Earth of the landslide and urban area southern the MMA. **b** Hillshade depicting the Olinalá landslide and other possible old landslides in the southern part of the MMA

bedrock. However, the failure boundary has not been defined or proved with certainty by geophysical data or drilling boreholes. Mass deposit is slightly segmented by very shallow runoffs, not the flanks that are cut by incisive rivers. This may imply a recent origin of the landslide since the main mass body has not been affected by significant surface erosion process. Landslide body is covered by trees and dry shrubs and grabs, some of which are tilted due to slow-displacement in instability direction. To date, there is no evidence of an active displacement of the entire mass, although minor cracks occur in some places along

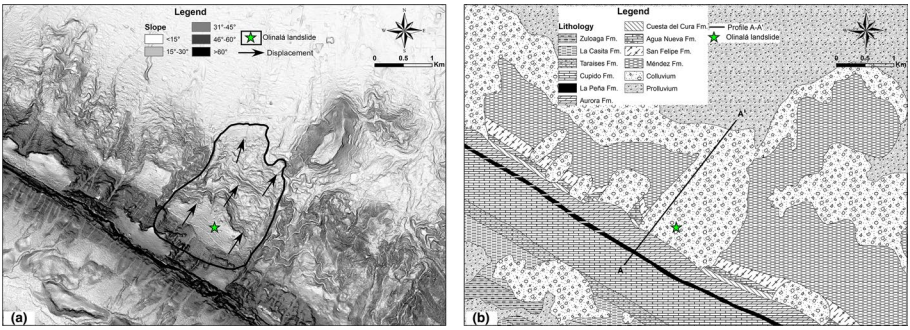

Fig. 6 Slope map (**a**) and lithological map (**b**) of the Olinalá landslide. Profile A–A' is depicted in Fig. 7

the landslide. Extreme rainfalls related with drastic climatic variations during the Quaternary have been proposed as the original trigger of the Olinalá landslide (Chapa Guerrero 1993), a similar explanation suggested for other ancient landslides located along the Monterrey Salient (Ruiz Martínez and Werner 1997). Nonetheless, such a supposition remains uncertain due to the lack of detailed studies debating the influence of other potential triggering agents. We suggest that some geomorphological features observed in the SMO are difficult to explain without considering a seismic origin. Although the Olinalá landslide seems stable under present-day conditions, recent small size landslide activity through the mass body is an indirect evidence of critical instability background on the slope. In addition, a reactivation would be very likely considering the moderate seismicity recorded in the region, a situation that may be exacerbated by the constant impact of storms (Ramos-Zuñiga et al. 2012b; Salinas-Jasso et al. 2017). Because the size and features of the sliding surface, which cut through the mountain top, it could be suggested the main slide was triggered by moderate to high magnitude seismicity instead of a solely saturated hydrological frame, as it has been proposed. Such features are recognized as topographic fingerprints of earthquake-induced landslides (Meunier et al. 2008; Wu et al. 2017). The following section discusses the stability analysis to test several scenarios considering different groundwater levels and a strong earthquake shaking.

5 Stability analysis

Our premise was to estimate likely conditions that could reactivate the Olinalá landslide. We have evaluated stability conditions both in static (aseismic) conditions and under a dynamic load (earthquake shaking). First estimation was derived from modeling failures surfaces considering several changes in groundwater conditions in the absence of earthquake shaking. On the other hand, estimation of stability conditions under a dynamic load includes modeling of earthquake shaking, considering ground acceleration. It has simulated an idealized configuration of the topography based on field inspection and the stratigraphic representation developed by Chapa Guerrero (1993) (Fig. 7). We used the SLIDE software (Rocscience Inc. 2002) to estimate the slope stability conditions and expected failure behavior for the explored scenarios. SLIDE calculates the factor of safety (FS), the ratio between resisting forces to driving forces facing slope instability, and possible failures depicted as circular or irregular slip surfaces in soils or rock slopes. A FS near to

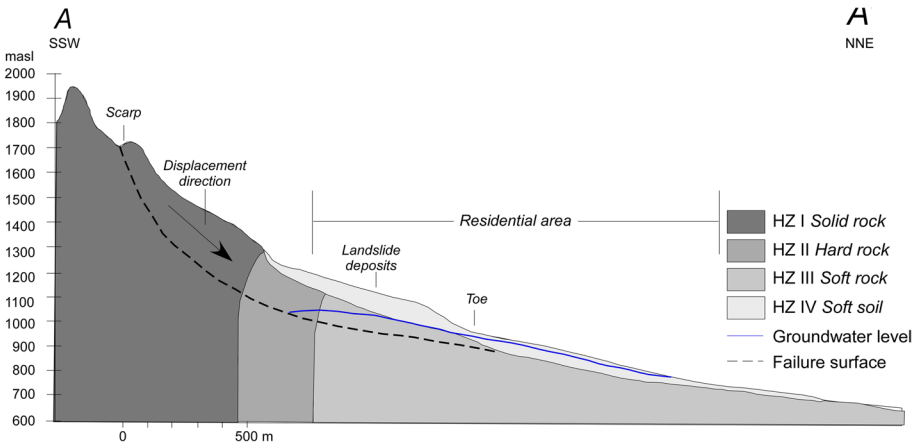

Fig. 7 Cross section of the Olinalá landslide (adapted from Chapa Guerrero 1993). Main features of the landslide are defined (scarp, deposit zone and toe). Colors represent the different homogeneous zones used in the stability analysis. Landslide boundary is depicted as a dashed line. Groundwater level is marked as the blue line. Residential zone refers to the region with the greatest amount of constructions and infrastructure over the landslide

1.0 defines a pseudostability condition through the slope assuming an imminent failure, whereas a FS greater than 1.0 indicates the slope is stable. We developed a bidimensional limit equilibrium analysis of the slope model applying the simplified Janbu method (Janbu 1954). Janbu's method satisfies both vertical and overall horizontal forces equilibrium for the entire slide mass, discarding a possible influence of interslice shear forces (Abramson et al. 2001). Failure boundary of the Olinalá landslide was fitted to the weathering zone in the basal mass body as proposed by Chapa Guerrero (1993). In order to deploy a straightforward representation, we have simplified the geological frame of the slope. The slope was subdivided into four lithological and geotechnical homogeneous zones (HZ) as proposed by Salinas-Jasso et al. (2019b): HZ I solid rock (carbonates), HZ II hard rock (carbonates and marls), HZ III soft rock (shales) and HZ IV soft soil (Quaternary deposits). Each homogeneous zone is defined by effective cohesion (c'), effective frictional angle (ϕ) and specific weight (γ) data as mentioned in the Table 2. Due to the impossibility to carry out detailed geotechnical test, representative shear strength values for each one of the HZ

Table 2 Average geotechnical data for the different lithological units in the study area

Lithological group	Description	c' (kN/m^2)	ϕ (º)	γ (kN/m^3)
Solid rock	Limestones with mudstone texture intercalated with marls and chert horizons	50	35	26
Hard rock	Sandstones, siltstones and shales	35	30	24
Soft rock	Conglomerates supported in a fine-grain matrix. Weathered shales	48	35	25
Soft soil	Unconsolidated alluvial deposits	24	32	18

Data from Chapa Guerrero (1993), Jaimes et al. (2013) and Salinas-Jasso et al. (2019b)

were assigned from a literature review and geotechnical data under professional judgment for the lithological groups in the study area (Chapa Guerrero 1993; Jaimes et al. 2013; Salinas-Jasso et al. 2019b). In order to estimate critical stability conditions on the slope, we used residual strengths in both static and dynamic scenarios.

Failures surfaces were estimated considering saturated groundwater conditions through the slope. Lack of published data made difficult modeling groundwater conditions. We suggested five groundwater levels and examined their effects on slope stability (Fig. 8). Groundwater levels were fitted according to the topographically driven flow assumption, which states that spatial distribution of the water table usually mimics the topography of the ground surface (Deming 2002). Such an estimation allows to calculate a generalized hydrogeological framework on the slope, preventing complex situations that could exist as several groundwater horizons or perched aquifers in the absence of in situ information. The first three cases depict a transitional decline of the groundwater level from a shallow position (Case 1 in Fig. 8) to a deeper position (Case 3 in Fig. 8), all of them interacting with the four HZ. Case 1 shows a groundwater level affecting the top of the HZ I and II, and the transition between the zones III and IV. Cases 2 and 3 are quite similar in the groundwater context. Case 2 depicts a groundwater level slightly above of the proposed Olinalá landslide boundary, affecting from the HZ I to III. On the other hand, case 3 shows the groundwater level slightly below the proposed failure surface. Case 4 depicts a groundwater level below the weathering zone of the limestone strata but above of the clayey materials, as

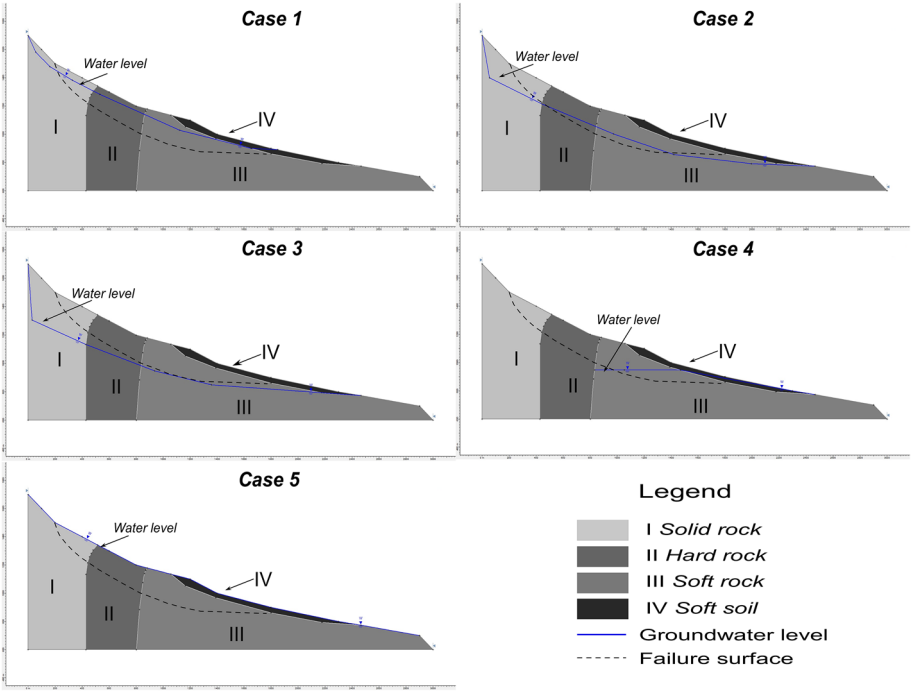

Fig. 8 Idealized groundwater conditions modeled in the slope stability analysis. Cases 1, 2, 3 and 5 show proposed water levels. Case 4 represent represents the groundwater level proposed by Chapa Guerrero (1993). Landslide boundary is depicted as a dashed line. Blue line shows the groundwater level. The numbers I, II, III and IV represent the homogenous zone used in the slope stability analysis

proposed by Chapa Guerrero (1993). Case 5 shows a groundwater level at the top of the slope, with seepage along the entire slope face. This hypothetical case would be the most critical situation here considered.

Seismic influence was estimated by a hypothetical M 6.5 earthquake. Epicenter was located at the same place of the San Pedro M 4.0 earthquake (January 2010, Fig. 4). Slope stability was modeled by applying a seismic load in horizontal direction and positive to direction of failure, keeping the same parameters as in the scenarios without earthquake shaking. For the seismic coefficient, we used peak ground acceleration (PGA) values calculated by Salinas-Jasso et al (2019b) from the ground motion prediction equations for extensional regimes derived by Pankow and Pechmann (2004). In this correlation, PGA value is in function of earthquake magnitude and the shorter distance in the bidimensional projection of the fault rupture on the surface. The attenuation relation is valid for both rock and soil sites, which allows calculate seismic site effects based on other seismic parameters, as V_{S30} value. For more details, the reader is encouraged to see Salinas-Jasso et al. (2019b). For the M 6.5 scenario, maximum ground accelerations would be 270 cm/s^2 and up to 350 cm/s^2 in close areas to the epicenter without and considering site effects in epicentral area, respectively. In the MMA valley, values range between 200–250 cm/s^2. For the study area, the average PGA values oscillate around the 300 cm/s^2. This value was chosen as the seismic coefficient required for modeling the dynamic response of the landslide, considering a less chance of landslide reactivation for the other PGA values (< 200 cm/s^2) obtained by Salinas-Jasso et al. (2019b). For both scenarios (aseismic and dynamic), SLIDE generated a wide variety of expected surfaces and calculated the factor of safety for each one of the failures.

6 Results

SLIDE generated several critical curved-surfaces, whose displacement occur under shear conditions through all the lithological sequence. Figures 9, 10, and 11 show all the surfaces for each one of the models. Legend is categorized in terms of the factor of safety, with red colors depicting critical stability conditions and up to a FS = 1.5 (blue colors), meaning an accepted stability state on the slope. It is important to mention that results should be only considered as an index and representation of potential instability under the modeled conditions.

For cases 1a, 2a and 3a, the minimum FS obtained were 0.8, 0.9 and 0.9, respectively (Fig. 9). These results did not consider any earthquake shaking influence, only groundwater level variations. For these cases, the expected failure surfaces have similar shapes. Case 1a shows critical stability conditions at the top of the slope, denoted by extended slip surfaces (red centers of slip circles) and linked to a shallow position of the water table. More stable conditions are randomly dispersed over the slope (see location of blue centers of slip circles in case 1a in Fig. 9). As groundwater level gets deeper in its position (from case 1a to case 3a), stability conditions are better, which is denoted by a predominance of slip surfaces with acceptable factors of safety (FS > 1.2, green circles) and a notably reduction of critical stability zones (red circles). For these cases, likely failure boundaries would affect all the sedimentary sequence, which would imply the occurrence of deep-seated slides. For the previous cases, factors of safety descend critically when the seismic influence (acceleration of 0.3 g) is invoked: 0.4, 0.4 and 0.5, respectively. Same, instability conditions are more severe. Failure surfaces under

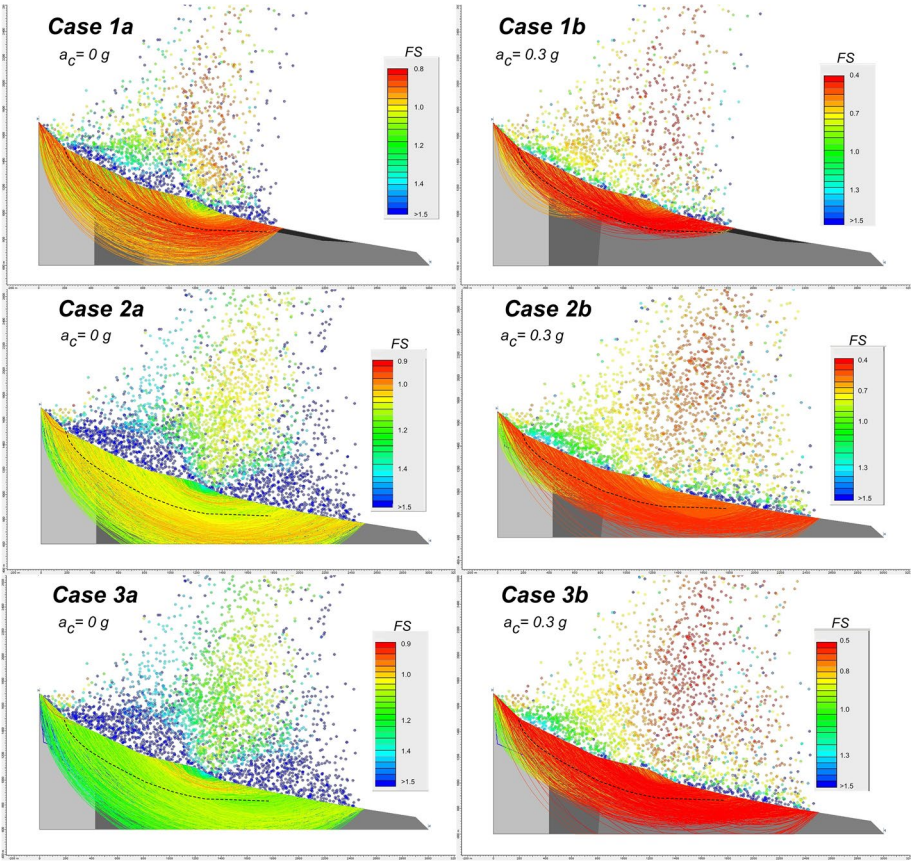

Fig. 9 Critical slip surfaces and their factors of safety for the cases 1 to 3. Left column shows modeled scenarios considering only variations in groundwater conditions. Right column depicts scenarios considering the influence of earthquake shaking. Dashed line defines the failure boundary

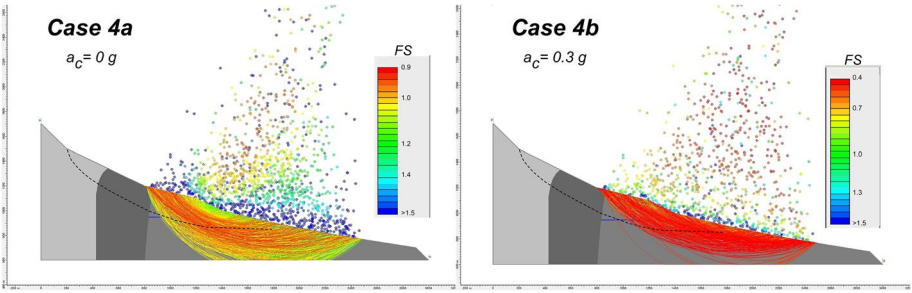

Fig. 10 Critical slip surfaces and their factors of safety for the case 4. Case 4a shows a model considering only groundwater conditions. Case 4b depicts expected failure surfaces considering the influence of earthquake shaking. Dashed line defines the failure boundary

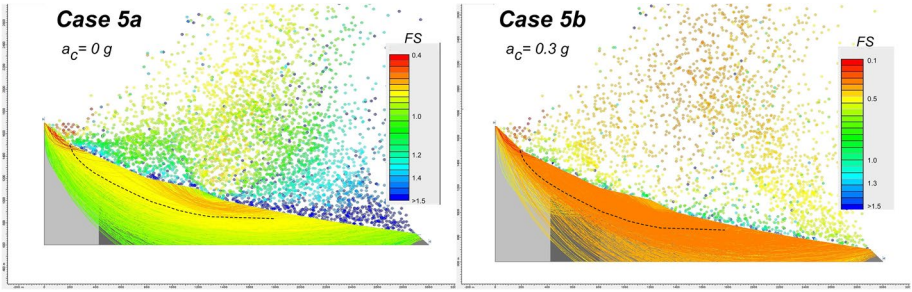

Fig. 11 Critical slip surfaces and their factors of safety for the case 5. Case 5a shows a scenario considering a drastic groundwater condition. Case 5b depicts failure surfaces considering the influence of earthquake shaking. Dashed line defines the failure boundary

dynamic conditions (cases 1b, 2b and 3b in Fig. 9) are shallower than the scenarios where only the hydrogeological variations were modeled (cases 1a to 3a). More surfaces stand out with FS < 1 compared to the analysis under static conditions. There is a remarkable prevalence of several surfaces with FS < 1.0 (green to red slip circles) for the three cases considering seismic conditions. Surfaces with FS > 1.5 (stable condition) are located towards the foothills, increasing in number from case 1b to case 3b (Fig. 9).

Case 4 depicts the hydrogeological conditions proposed by Chapa Guerrero (1993) (Fig. 10). Failure surfaces without earthquake shaking mainly affect the marl-shale sequence characterized by the San Felipe and Méndez formations as well as the Quaternary deposits (HZ III and HZ IV, respectively). Minimum factor of safety obtained for this estimation was 0.9, with several slip surfaces with FS > 1.3 (green to blue circles, case 4a in Fig. 10). Critical stability conditions (red circles) are similar and located near the groundwater position, extending from the middle part towards the bottom of the slope, involving only the lower part of the Olinalá landslide. Solid (HZ I) and hard rock (HZ II) groups are not affected by likely unstable surfaces under this hydrogeological condition. Surfaces with FS > 1.5 are shallower through the mass body. Taking into account the seismic acceleration, minimum factor of safety was 0.4 (case 4b in Fig. 10). It is remarkable the decrease of potential stable surfaces (FS > 1.5, blue circles) and a huge increase of critical slip surfaces (green to red circles). Likely failure surfaces are very shallow, suggesting displacement through all the weathering deposits and the top of the bedrock as shallow slides. For this case is clear that carbonate sequence would not be affected by instability conditions.

The most critical scenario would be the case 5 (Fig. 11). Here, it has been proposed the groundwater rise above the aquifer and flow onto all the slope face. For this condition and discarding an earthquake, minimum factor of safety obtained was 0.4 (case 5a in Fig. 11). Practically all the slope presents critical stability conditions, which is depicted by several surfaces with FS < 1. A critical situation is identified on the top of the slope in the HZ I, with very shallow critical surfaces. This situation could produce shallow rock slides and rock avalanches. Potential surfaces with highest factors of safety are near the surface, but prevail at the bottom of the slope (blue circles). Such a situation, expected under saturated conditions, would predispose a dramatic scenarios of landslides activation. When the seismic load is applied, the likely failures are not so different in shape compared to the previous scenario (case 5b in Fig. 11). Earthquake shaking would destabilize the slope, including those portions that remained fairly stable

without seismic influence. Factor of safety descends from 0.4 to 0.1, the lowest FS value obtained for all the scenarios analyzed. Failures surfaces with FS > 1.5 are very few.

Cases 1 to 4 are characterized by critical stability slope conditions, but slightly stable under the hydrogeological context proposed. Surfaces geometry are mainly controlled by the groundwater depth and location. Considering a seismic influence, the slope would be predisposing to drastic landslide (re)activations, most prominent in cases 1 to 3 and located for case 4. Case 5 exhibits null stability conditions on the slope. Presence of a water level flowing on the surface and the moderate earthquake shaking would depict a critical triggering mechanism for slope instability. However, the simple fact of considering a surface water table is unrealistic and unlikely in the study area.

It seems possible a reactivation of the Olinalá landslide under the estimated conditions: a saturated hydrogeological context and a moderate ground shaking. However, some constraints could be mentioned based on the results. When stability analysis is estimated based only in the groundwater context and discarding earthquake shaking, FS for cases 1 to 4 represent critical instability conditions (FS = 0.8, 0.9, 0.9 and 0.9, respectively), which could initiate a slope creep movement instead of a rapid and destructive failure of the slide. Situation would be quite different for the case 5a (FS = 0.4) and all the cases considering earthquake shaking, where FS drops sharply (FS = 0.4, 0.4, 0.5, 0.4, and 0.1, respectively). The analysis showed the estimated scenarios are sensitive when earthquake shaking is considered in the modeling. A moderate ground shaking associated with a M 6.5 earthquake, producing PGA of 0.3 g, would have the potential to reactivate the Olinalá landslide and trigger several additional shallow and deep-seated slides as well as flows and avalanches, predisposing a catastrophic scenario on the slope. A likely reactivation of the Olinalá landslide would be possible in cases 1, 2 and 3, both in static and dynamic conditions. Case 4 depicts a potential reactivation only of located zones through the landslide (middle and lower portions). Although case 5 would represent the worst scenario expected under the modeled conditions, the fact of its almost unlikely representation rules it out as a dangerous situation in the study area.

Salinas-Jasso et al. (2019b) developed a landslide hazard zonation in the MMA. Regional maps predicting the expected areal limits for potential earthquake-induced landslides in terms of coseismic displacements were generated for several earthquake scenarios. Based on their results, the Olinalá landslide is located in a hazardous zone. Expected coseismic displacement could reach 5 cm up to 10 cm. Such a displacement range causes most of the soils loss significant amount of shear strength, even decreasing to residual strength conditions, and therefore failure (Jibson and Keefer 1993). According with this, catastrophic rock avalanches and rapid soil flows, two of the landslides with high death rates (Keefer 2002), would be very likely.

The behavior of such catastrophic failures would be uncertain. In this condition, deep-seated slides are also possible, affecting the thick sequence of Quaternary deposits and the weathering zone of rock formations. A rapid reactivation of the landslide and generation of new failures, would involve significant damage due urbanization on the slope and in the foothills. Potential affected area is populated by close to 10,000 inhabitants and is host to a large number of shopping, transportation and financial centers as well as health and educational institutions (INEGI 2019). Damage could be higher by damming rivers and related floodings (Salinas-Jasso et al. 2019b). Liquefaction processes would be expected, mainly on the middle and bottom of the mass body, which could reduce the strength of the slope materials and might induce failures. Highways and critical lifelines would be disrupted, avoiding fast response by rescue and emergency departments in critical situations. Potential reactivations of some portions through the landslide can be promoted by the constant

anthropogenic activity, mainly at the hillslope toe. Reactivations could be related to human intervention by construction and related deforestation on marginally stable slope sections, where new settlements are being built. It can be speculated, with great accuracy, that most newcomers and developers do not even know of the presence of the landslide, underestimating the real impact that their intervention may induce in the slope stability, as it has been the case in other sites in the MMA (Montalvo-Arrieta et al. 2010).

7 Discussion

Recent studies have showed a clear evidence of large paleo-landslides in the mountains bordering the MMA, which have been urbanized by the disordered city growth. Due to the latent risk in which people live, is imperative to know what conditions may reactivate such mass movements. Landslides induced by a combined effect of rainfall and earthquakes are not rare. Several examples are reported around the world (Sassa et al. 2007; Palmer 2017). The most recent case occurred in Japan in September 2018. On September 6, a M 6.7 earthquake struck the Hokkaido island, generating a widespread devastation and damage (Normile 2018). The earthquake induced almost 6,000 shallow landslides, killing 36 persons (Yamagishi and Yamazaki 2018). Despite the moderate ground shaking, there is no doubt most of the japanese mountain regions were much susceptible to landslides in the aftermath of the powerful Typhoon Jebi, just a few days before the earthquake struck the Japan's land region.

Our results suggest the Olinalá landslide would present unfavorable stability conditions under the simulated scenarios. Extraordinary rainfalls by major hurricanes and tropical storms discharge large amount of water through the region. However, there is no evidence between these events and a reactivation of the Olinalá landslide. Only small shallow slides, debris flows and rockfalls have been constant along the mass body after extraordinary rainfalls. This pattern has been recognized in other places around the world where it has been observed that intense rainfalls cause several small landslides over a wide area but not deep-seated rock slides, which need major changes in the groundwater regime (Densmore and Hovius 2000; Hancox and Perrin 2009). Despite the great amount of precipitation discharged by storms, it would be important to quantify how much of this water is directly infiltrated into the Olinalá landslide. It could be assumed that most of the precipitated water flows on the slope by the presence of roads, transportation routes and buildings related with the urbanization process of the city, becoming the terrain impervious. Other factors, related with the failure surface features (geometry and location related to the groundwater level) should be examined in detail from geotechnical surveys and drilling boreholes to characterize a more realistic context of the slope stability for several paleo-landslides located through the SMO. An analysis of the landslide displacement should be developed either with field techniques or satellite-based estimations.

Predict a potential displacement in a landslide is difficult. A main challenge is evaluating under what conditions a quite-slow landslide will change its behavior from a stable state to an upcoming displacement rapid event, and if those triggering conditions are likely to occur in the area of concern. Despite the low to moderate magnitude of seismicity in northeastern Mexico, the occurrence of more powerful earthquakes is known (Galván-Ramírez and Montalvo-Arrieta 2008; Ramos-Zuñiga et al. 2012b). Evidence of historical major earthquakes in northeastern Mexico (see Sect. 2.4) suggests an alarming potential of a similar earthquake in the future, when cities will have more

infrastructure and population. Zúñiga et al. (2017) developed a seismic regionalization of Mexico for seismic hazard and risk analyses. For the northeastern Mexico, they estimated a recurrence interval of 104 years for earthquakes with magnitudes $M \geq 6.5$, based on the fact that there is no evidence of moderate to stronger events during the last century. Several authors (Muehlberger et al. 1978; McKee et al. 1984; Aranda-Gómez et al. 2005) have proposed different reactivation lapses of ancient basement faults (e.g., San Marcos and La Babia faults), which it has been assumed as a possible explanation for seismicity in northeastern Mexico (Ramos-Zuñiga et al. 2012b). In order to evaluate the seismogenic potential in the region, further detailed-studies should be deployed. This has forced development of zonations to evaluate seismic-induced hazard and damage quickly after an earthquake occurs (Montalvo-Arrieta et al. 2011; Salinas-Jasso et al 2019b). Such maps can be used as input data in future detailed risk assessments, facing emergency contingencies as well as design of regulations for building codes in cities located in continental interiors, as in the case of those settled in northeastern Mexico.

8 Conclusions

We developed a dynamic analysis to evaluate the stability conditions of the Olinalá landslide, a paleo-landslide located in the front of the Sierra Madre Oriental and that has been covered by the urban growth of the Monterrey Metropolitan Area. The stability analysis was based on the modeling of several hydrogeological conditions as well as a seismic scenario. Our results show that under the current hydrological and geological conditions, the Olinalá landslide has a low probability of reactivation. Involving seismicity, for the first time, suggests an additional force required to trigger displacement along all the landslide. Hence, it is recommended to develop detailed studies and early prevention strategies to cope to an unexpected reactivation, both shallow slides or all the mass body. The possibility of a reactivation under a combined effect of rainfall-earthquake should be considered even for low-to-moderate magnitude earthquakes. Additionally, detailed field inspection and ground-based monitoring techniques are highly desired in order to identify a more realistic context on the landslide, although satellite techniques could be helpful for the purpose. This kind of assessment could be applied in other regions of the Sierra Madre Oriental where several towns are settled and have been affected by seismic shaking. Our results constitute a useful information in order to develop a landslide risk assessment for the study area in the near future. In conjunction with detailed landslide susceptibility and landslide hazard assessments, the analysis presented here can be used for the construction of risk scenarios and evaluate expected damage if an unexpected reactivation take place. Such evaluations could be involved in urban city planning, delimiting stable zones for construction and adequate prevention or mitigation measures to cope with landslides.

Acknowledgements First author received a scholarship from Consejo Nacional de Ciencia y Tecnología (CONACYT). The authors are grateful to Thomas Glade, Editor in Chief, and two anonymous reviewers for their critical remarks that helped to greatly improve the original manuscript.

Compliance with ethical standards

Conflict of interest The authors declare that they have no conflict of interest.

References

Abramson LW, Lee TS, Sharma S, Boyce GM (2001) Slope stability and stabilization methods, 2nd edn. Wiley, London

Alcántara-Ayala I (2002) Geomorphology, natural hazards, vulnerability and prevention of natural disasters in developing countries. Geomorphology 47:107–124

Aranda-Gómez JJ, Housh TB, Luhr JF, Henry CD, Becker T, Chávez-Cabello G (2005) Reactivation of the San Marcos fault during mid to late Tertiary extension, Chihuahua, Mexico. In: Anderson TH, Nourse JA, McKee JW, Steiner MB (eds) The Mojave-Sonora megashear hypothesis: development, assessment, and alternatives. Geological Society of America Special Paper 393, pp 509–521

Bird JF, Bommer J (2004) Earthquake losses due to ground failure. Eng Geol 75:147–179

Casagli N, Cigna F, Bianchini S, Hölbling D, Füreder P, Righini G, Del Conte S, Friedl B, Schneiderbauer S, Iasio C, Vlcko J, Greif V, Proske H, Granica K, Falco S, Lozzi S, Mora O, Arnaud A, Novali F, Bianchi M (2016) Landslide mapping and monitoring by using radar and optical remote sensing: examples from the EC-FP7 project SAFER. Remote Sens Appl: Soc Environ 4:92–108

Cascini L, Fornaro G, Peduto D (2010) Advanced low- and full-resolution DInSAR map generation for slow-moving landslide analysis at different scales. Eng Geol 112:29–42

Carrara A, Guzzetti F, Cardinali M, Reichenbach P (1999) Use of GIS technology in the prediction and monitoring of landslide hazard. Nat Hazards 20:117–135

Chapa Guerrero JR (1993) Massenbewegungen an steilhängen der Sierra Madre Oriental im grossraum Monterrey, Mexiko. Dissertation, RWTH Aachen University, Germany

Chávez-Cabello G, Aranda-Gómez JJ, Molina-Garza RS, Cossío-Torres T, Arvizu-Gutiérrez IR, González-Naranjo GA (2005) La falla de San Marcos: una estructura jurásica de basamento multirreactivada del noreste de México. Bol Soc Geol Mex 57:27–52

CONAGUA (2010) Reseña del huracán "Alex" del Oceáno Atlántico. Coordinación General del Servicio Meteorológico Nacional, 13

CONAGUA (2012) Base de datos de ciclones tropicales que impactaron a México de 1970 a 2011. Coordinación General del Servicio Meteorológico Nacional, 7

CONAGUA (2018) Actualización de la disponibilidad media anual de agua en el acuífero Área Metropolitana de Monterrey (1906), Estado de Nuevo León. Diario Oficial de la Federación, 37

CONAGUA (2019) Weather information (online): https://smn.cna.gob.mx/es/climatologia/informacion-climatologica. Last access Oct 2019

Corominas J, Moya J, Ledesma A, Lloret A, Gili JA (2005) Prediction of ground displacements and velocities from groundwater level changes at the Vallcebre landslide (Eastern Pyrenees, Spain). Landslides 2:83–96

Corominas J, van Westen C, Frattini P, Cascini L, Malet JP, Fotopoulou S, Catani F, Van Den Eeckhaut M, Mavrouli O, Agliardi F, Pitilakis K, Winter MG, Pastor M, Ferlisi S, Tofani V, Hervás J, Smith JT (2014) Recommendations for the quantitative analysis of landslide risk. Bull Eng Geol Environ 73(2):209–263

Dai FC, Lee CF, Ngai YY (2002) Landslide risk assessment and management: an overview. Eng Geol 64:65–87

De León-Gómez H, Masuch-Oesterreich D, Medina-Barrera F, Hellweg F (1998) Investigaciones hidrogeológicas en el Cañón de la Huasteca como contribución al abastecimiento de agua potable de Monterrey, Nuevo León, México. Geogaceta 23:87–90

Deming D (2002) Introduction to hydrogeology. McGraw-Hill, New York, p 468

Densmore AL, Hovius N (2000) Topographic fingerprints of bedrock landslides. Geology 28(4):371–374

Dewitte O, Chung CJ, Demoulin A (2006) Reactivation hazard mapping for ancient landslides in West Belgium. Nat Hazards Earth Syst Sci 6:653–662

Dickinson WR, Lawton T (2001) Carbonaceous to Cretaceous assembly and fragmentation of Mexico. Geol Soc Am Bull 113:1142–1160

Doser DI (1987) The 16 August 1931 Valentine, Texas, earthquake: evidence for normal faulting in west Texas. Bull Seismol Soc Am 77:2005–2017

Doser DI, Rodríguez J (1993) The seismicity of Chihuahua, Mexico, and the 1928 Parral earthquake. Phys Earth Planet Inter 78:97–104

Eguiluz de Antuñano S, Aranda García M, Marret R (2000) Tectónica de la Sierra Madre Oriental. Bol Soc Geol Mex 53:1–26

Fell R, Corominas J, Bonnard C, Cascini L, Leroi E, Savage WZ (2008) Guidelines for landslide susceptibility, hazard and risk zoning for land use planning. Eng Geol 102:85–98

Fitz-Díaz E, Lawton TF, Juárez-Arriaga E, Chávez-Cabello G (2018) The Cretaceous-Paleogene Mexican orogen: structure, basin, development, magmatism and tectonics. Earth Sci Rev 183:56–84

Frohlich C, Davis SD (2002) Texas earthquakes. Springer, Berlin, p 277
Galván-Ramírez IN, Montalvo-Arrieta J (2008) The historical seismicity and prediction of ground motion in northeast Mexico. J S Am Earth Sci 25:37–48
García Acosta V, Suárez Reynoso G (1996) Los sismos en la historia de México. Universidad Nacional Autónoma de México, México
Gómez-Arredondo CM, Montalvo-Arrieta J, Iglesias-Mendoza A, Espindola-Castro V (2016) Relocation and seismotectonic interpretation of the seismic swarm of August–December of 2012 in the Linares area, northeastern Mexico. Geofís Int 55(2):95–106
Guzzetti F, Mondini AC, Cardinali M, Fiorucci F, Santangelo M, Chang KT (2012) Landslide inventory maps: new tools for an old problem. Earth Sci Rev 112:42–66
Hancox GT, Perrin ND (2009) Green Lake landslide and other giant and very large postglacial landslides in Fiordland, New Zealand. Quat Sci Rev 28:1020–1036
INEGI (2019) Population data (online): https://www.inegi.org.mx. Last access Oct 2019
Intrieri E, Raspini F, Fumagalli A, Lu P, Del Conte S, Farina P, Allievi J, Ferreti A, Casagli N (2017) The Maoxian landslide as seen from space: detecting precursors of failure with Sentinel-1 data. Landslides 15(1):123–133
Jaimes MA, Niño M, Reinoso E (2013) Una aproximación para la obtención de mapas de desplazamiento traslacional de laderas a nivel regional inducidos por sismos. Rev Ing Sísm 89:1–23
Janbu N (1954) Application of composite slip surface for stability analysis. In: European conference on stability of earth slopes. Stockholm, Sweden
Jáuregui E (2003) Climatology of landfalling hurricanes and tropical storms in Mexico. Atmósfera, 193–204.
Jibson RW, Keefer DK (1993) Analysis of the seismic origin of landslides: examples from the New Madrid seismic zone. Geol Soc Am Bull 105:521–536
Jibson RW, Harp E, Michael A (2000) A method for producing digital probabilistic seismic landslide hazard maps. Eng Geol 58:271–289
Keefer DK (2002) Investigating landslides caused by earthquakes: a historical review. Surv Geophys 23:473–510
Korup O, Densmore AL, Schlunegger F (2010) The role of landslides in mountain range evolution. Geomorphology 120:77–90
Legorreta Paulin G, Bursik M, Lugo-Hubp J, Zamorano Orozco JJ (2010) Effect of pixel size on cartographic representation of shallow and deep-seated landslide, and its collateral effects on the forecasting of landslide by SINMAP and Multiple Logistic Regression landslide models. Phys Chem Earth 35:137–148
Mansour MF, Morgenstern NR, Martin C (2011) Expected damage from displacement of slow-moving slides. Landslides 8:117–131
Martini M, Ortega-Gutiérrez F (2018) Tectono-stratigraphic evolution of eastern Mexico during the break-up of Pangea: a review. Earth Sci Rev 183:38–55
Massey CI, Petley DN, McSaveney MJ (2013) Patterns of movements in reactivated landslides. Eng Geol 159:1–19
McKee JW, Jones NW, Long LE (1984) History of recurrent activity along a major fault in northeastern Mexico. Geology 12(2):103–107
Metternicht G, Hurni L, Gogu R (2005) Remote sensing of landslides: an analysis of the potential contribution to geo-spatial systems for hazard assessment in mountainous environments. Remote Sens Environ 98:284–303
Meunier P, Hovius N, Haines JA (2008) Topographic site effects and the location of earthquake induced landslides. Earth Planet Sci Lett 275:221–232
Molina-Garza RS, Iriondo A (2005) La megacizalla Mojave-Sonora: la hipótesis, la controversia y el estado actual de conocimiento. Bol Soc Geol Mex 57:1–26
Montalvo-Arrieta JC, Chávez-Cabello G, Velasco-Tapia F, Navarro de León I (2010) Causes and effects of landslides in the Monterrey Metropolitan Area, NE Mexico. In: Werner ED, Friedman H (eds) Landslides: causes, types and effects. Nova Science Publishers, New York, pp 72–104
Montalvo-Arrieta JC, Ramos-Zuñiga LG, Navarro de León I, Ramírez-Fernández JA (2011) Una aproximación a la regionalización sísmica del estado de Nuevo León, basada en velocidades de propagación de ondas de corte y geología. Bol Soc Geol Mex 63(2):217–233
Montalvo-Arrieta JC, Sosa-Ramírez RL, Paz-Martínez EG (2015) Relationship between MMI data and ground shakingin the state of Nuevo León. Northeastern Mexico Seismol Res Lett 86(5):1–7
Montalvo-Arrieta JC, Pérez-Campos X, Ramos-Zuñiga LG, Paz-Martínez EG, Salinas-Jasso JA, Navarro de León I, Ramírez-Fernández JA (2018) El Cuchillo seismic sequence of October 2013–July 2014

in the Burgos Basin, northeastern Mexico: hydraulic fracturing or reservoir-induced seismicity? Bull Seismol Soc Am 108(5B):3092–3106
Muehlberger WR, Belcher RC, Goetz LK (1978) Quaternary faulting in Trans-Pecos Texas. Geology 6(6):337–340
Muñiz-Jauregui JA, Hernández-Madrigal VM (2012) Zonificación de procesos de remoción en masa en Puerto Vallarta, Jalisco, mediante combinación de análisis multicriterio y método heurístico. Rev Mex Cien Geol 29:103–114
Murillo-García FG, Steger S, Alcántara-Ayala I (2019) Landslide susceptibility: a statistically-based assessment on a depositional pyroclastic ramp. J Mt Sci 16(3):561–580
Natali SG, Sbar ML (1982) Seismicity in the epicentral region of the 1887 northeastern Sonora earthquake, Mexico. Bull Seismol Soc Am 72:181–196
Normile D (2018) Slippery volcanic soils blamed for deadly landslides during Hokkaido earthquake. Science. https://doi.org/10.1126/science.aav3821
Padilla y Sánchez RJ (1985) Las estructuras de la curvatura de Monterrey, estados de Coahuila, Nuevo León, Zacatecas y San Luis Potosí. Rev Inst de Geol 6:1–20
Palmer J (2017) Creeping earth could hold secret to deadly landslides. Nature 548:384–386
Pankow KL, Pechmann JC (2004) The SEA99 ground-motion predictive relations for extensional tectonic regimes: revisions and a new peak ground velocity relation. Bull Seismol Soc Am 94:341–348
Petley D (2012) Global patterns of loss of life from landslides. Geology 40(10):927–930
Ramos-Zuñiga LG, Montalvo-Arrieta JC, Pérez-Campos X, Váldes-González C (2012a) Seismic characterization of station LNIG as a reference site in northeast Mexico. Geofís Int 51:185–195
Ramos-Zuñiga LG, Medina-Ferrusquía H, Montalvo-Arrieta J (2012b) Patrones de sismicidad en la curvatura de Monterrey, noreste de México. Rev Mex Cienc Geol 29(2):572–589
Rocscience Inc. (2002) Slide 2D limit equilibrium slope stability for soil and rock slopes. User's guide
Ruiz Martínez MA, Werner J (1997) Research into the quaternary sediments and climatic variation in NE Mexico. Quat Int 43(44):145–151
Salinas-Jasso JA, Salinas-Jasso RA, Montalvo-Arrieta JC, Alva-Niño E (2017) Inventario de movimientos en masa en el Sector Sur de la Saliente de Monterrey. Caso de estudio: Cañón Santa Rosa, Nuevo León (Noreste de México). Rev Mex Cienc Geol 34(3):182–198
Salinas-Jasso JA, Montalvo-Arrieta JC, Reinoso-Angulo E (2018) Landslides induced by a low seismic sequence at continental interiors: a case study of the Santa Rosa canyon, northeastern Mexico. Landslides 15:783–795
Salinas-Jasso JA, Montalvo-Arrieta JC, Alva-Niño E, Navarro de León I, Gómez-González JM (2019a) Seismic site effects in the central zone of Monterrey Metropolitan Area (Northeast Mexico) from a geotechnical-multidisciplanary assessment. Bull Eng Geol Environ 78(1):483–495
Salinas-Jasso JA, Ramos-Zuñiga LG, Montalvo-Arrieta JC (2019b) Regional landslide hazard assessment from seismically induced displacements in Monterrey Metropolitan area. Northeastern Mexico Bull Eng Geol Environ 78(2):1127–1141
Sassa K, Fukuoka H, Wang F, Wang G (2007) Landslides induced by a combined effect of earthquake and rainfall. In: Sassa K, Fukuoka H, Wang F, Wang G (eds) Progress in landslides science. Springer, Berlin
Shahabi H, Hashim M (2015) Landslide susceptibility mapping using GIS-based statistical models and remote sensing data in tropical environment. Sci Rep 5:9899
Van Asch ThWJ, Van Beek LPH, Bogaard TA (2007) Problems in predicting the mobility of slow-moving landslides. Eng Geol 91:46–55
Van Den Eeckhaut M, Poesen J, Dewitte O, Demoulin A, De Bo H, Vanmaercke-Gottigny MC (2007) Reactivation of old landslides: lessons learned from a case-study in the Flemish Ardennes. Soil Use Manag 23:200–211
Villaseñor-Reyes CI, Dávila-Harris P, Hernández-Madrigal VM, Figueroa-Miranda S (2018) Deep-seated gravitational slope deformations triggered by extreme rainfall and agricultural practices (eastern Michoacan, Mexico). Landslides 15:1867–1879
Wu G, Cunningham D, Yuan R, Zhou Q, Zeng X, Yang X (2017) Mass-wasting effects induced by the 2015 Gorkha (Nepal) Mw 7.8 earthquake within a large paleo-landslide site adjacent to the Tatopani Border Station, Nepal: implications for future development along the critical Bhote Koshi River valley transport corridor between Nepal and China. Landslides 14:1147–1160
Xie J (1998) Spectral inversion of Lg from earthquakes: a modified method with applications to the 1995, Western Texas earthquake sequence. Bull Seismol Soc Am 88:1525–1537
Yamagishi H, Yamazaki F (2018) Landslides by the 2018 Hokkaido Iburi-Tobu earthquake on September 6. Landslides 15(12):2521–2524

Zúñiga FR, Suárez G, Figueroa-Soto A, Mendoza A (2017) A first-order seismotectonic regionalization of Mexico for seismic hazard and risk estimation. J Seismol 21(6):1295–1322